Video Article

In Situ Synthesis of Gold Nanoparticles without Aggregation in the Interlayer Space of Layered Titanate Transparent Films

Kazuhisa Sasaki[1], Kazuki Matsubara[1], Shiori Kawamura[1], Kenji Saito[1], Masayuki Yagi[1], Tatsuto Yui[1]

[1]Department of Material Science and Technology, Faculty of Engineering, Niigata University

Correspondence to: Tatsuto Yui at yui.t@eng.niigata-u.ac.jp

URL: https://www.jove.com/video/55169
DOI: doi:10.3791/55169

Keywords: Engineering, Issue 119, Layered Semiconductor Films, Metal Nanoparticles, Gold Nanoparticles, Titania Nanosheets, Intercalation, Inorganic-Inorganic Hybrid Materials, Transparent Film

Date Published: 1/17/2017

Citation: Sasaki, K., Matsubara, K., Kawamura, S., Saito, K., Yagi, M., Yui, T. *In Situ* Synthesis of Gold Nanoparticles without Aggregation in the Interlayer Space of Layered Titanate Transparent Films. *J. Vis. Exp.* (119), e55169, doi:10.3791/55169 (2017).

Abstract

Combinations of metal oxide semiconductors and gold nanoparticles (AuNPs) have been investigated as new types of materials. The *in situ* synthesis of AuNPs within the interlayer space of semiconducting layered titania nanosheet (TNS) films was investigated here. Two types of intermediate films (*i.e.,* TNS films containing methyl viologen (TNS/MV^{2+}) and 2-ammoniumethanethiol (TNS/2-AET^{+})) were prepared. The two intermediate films were soaked in an aqueous tetrachloroauric(III) acid ($HAuCl_4$) solution, whereby considerable amounts of Au(III) species were accommodated within the interlayer spaces of the TNS films. The two types of obtained films were then soaked in an aqueous sodium tetrahydroborate ($NaBH_4$) solution, whereupon the color of the films immediately changed from colorless to purple, suggesting the formation of AuNPs within the TNS interlayer. When only TNS/MV^{2+} was used as the intermediate film, the color of the film gradually changed from metallic purple to dusty purple within 30 min, suggesting that aggregation of AuNPs had occurred. In contrast, this color change was suppressed by using the TNS/2-AET^{+} intermediate film, and the AuNPs were stabilized for over 4 months, as evidenced by the characteristic extinction (absorption and scattering) band from the AuNPs.

Video Link

The video component of this article can be found at https://www.jove.com/video/55169/

Introduction

Various noble metal nanoparticles (MNPs) exhibit characteristic colors or tones due to their localized surface plasmon resonance (LSPR) properties; thus, MNPs can be used in various optical and/or photochemical applications[1-4]. Recently, combinations of metal oxide semiconductor (MOS) photocatalysts, such as titanium oxide (TiO_2) and MNPs, have been thoroughly investigated as new types of photocatalysts[5-14]. However, in many cases, very small amounts of MNPs exist on the MOS surface, because most MOS particles have relatively low surface areas. On the other hand, layered metal oxide semiconductors (LMOSs) exhibit photocatalytic properties and have a large surface area, typically several hundred square meters per unit g of an LMOS[15-17]. In addition, various LMOSs have intercalation properties (*i.e.,* various chemical species can be accommodated within their expandable and large interlayer spaces)[15-20]. Thus, with a combination of MNPs and LMOSs, it is expected that relatively large amounts of MNPs are hybridized with the semiconductor photocatalysts.

We have reported the first *in situ* synthesis of copper nanoparticles (CuNPs)[21] within the interlayer space of LMOS (titania nanosheet; TNS[16-30]) transparent films through very simple steps. However, the details of the synthetic procedures and the characterization of the other noble MNPs and TNS hybrids have not yet been reported. Moreover, the CuNPs within the TNS layers were easily oxidized and decolorized under ambient conditions[21]. As such, we focused on gold nanoparticles (AuNPs), because AuNPs are widely used for various optical, photochemical, and catalytic applications, and it is expected that they will be relatively stable against oxidation[3-5,7,8,10-14,28,31,32]. Here, we report the synthesis of AuNPs within the interlayer space of TNS and show that 2-ammoniumethanethiol (2-AET^{+}; **Figure 1** inset) works effectively as a protective reagent for AuNPs within the interlayer of TNS.

Protocol

Caution: Always use caution when working with chemicals and solutions. Follow the appropriate safety practices and wear gloves, glasses, and a lab coat at all times. Be aware that nanomaterials may have additional hazards as compared to their bulk counterpart.

1. Preparation of Regents

1. Prepare the methyl viologen aqueous solution by dissolving 0.0012 g of 1,1'-dimethyl-4,4'-bipyridinium dichloride (methyl viologen; MV^{2+}) in 20 ml of water to give 0.2 mM MV^{2+}.

2. Prepare the gold(III) chloride aqueous solution by dissolving 0.1050 g of gold(III) tetrachloride trihydrate ($HAuCl_4 \cdot 3H_2O$) in 10 ml of water to give 25 mM $HAuCl_4$.
3. Prepare the sodium borohydride aqueous solution by dissolving 0.03844 g of sodium tetrahydroborate ($NaBH_4$) in 10 ml of water to give 100 mM $NaBH_4$.
4. Prepare the 2-ammoniumethanethiol aqueous solution by dissolving 0.2985 g of 2-ammoniumethanethiol chloride salt ($2\text{-}AET^+$) in 25 ml of water to give 100 mM $2\text{-}AET^+$.

2. Synthesis of TNS Colloidal Suspensions

NOTE: Titania nanosheets (TNS; $Ti_{0.91}O_2$) were prepared according to the well-established procedure reported previously[22,23,30].

1. Prepare the starting material of layered cesium titanate $Cs_{0.7}Ti_{1.825}O_4$ by calcining a stoichiometric mixture of Cs_2CO_3 (0.4040 g) and TiO_2 (ST-01; 0.5000 g) at 800 °C for 20 hr[22]. Repeat this twice.
2. Prepare the protonated layered titanate ($H_{0.7}Ti_{1.825}O_4 \cdot H_2O$) by repeatedly treating 0.8142 g of cesium titanate with an HCl (100 mM, 81.42 ml) aqueous solution by using a shaker (300 Hz) for 12 hr.
3. Prepare the exfoliated layered titanate (TNS) colloidal suspensions by stirring the protonated titanate powder (0.0998 g) vigorously (500 rpm) with 25 ml of a 17 mM tetrabutylammonium hydroxide ($TBA^+ OH^-$) aqueous solution for about 2 weeks at ambient temperature under dark conditions. The resulting opalescent suspension contains exfoliated titania nanosheets (TNS; 1.4 g/L, pH = 11~12).

3. Synthesis of TNS Films[21]

1. **Preparation of TNS cast films (c-TNS)**
    1. Pre-clean glass substrates (~20 x 20 mm^2) through ultrasonic treatments using an ultrasonic cleaner (27 kHz) in 1 M aqueous sodium hydroxide (NaOH) for 30 min.
    2. Rinse the substrates with 5-10 mL of ultrapure water (<0.056 μS cm^{-1}).
    3. Dip a glass substrate in a 0.1 M aqueous hydrochloric acid (HCl) for 3 min and rinse with 5-10 ml of ultrapure water.
    4. Clean the substrates through ultrasonic treatments (27 kHz) in pure water for 1 hr, and then rinse with pure water. Dry with a hairdryer for 2-3 min (until dry).
    5. Cast the colloidal suspension of TNS on the glass substrate in 300 μl aliquots.
    6. Dry at 60 °C for 2 hr using a dry oven to give the c-TNS film.

2. **Preparation of Sintered TNS Film (s-TNS)**
    1. To achieve thermal fixation of the TNS components on the glass substrate (s-TNS film), sinter the obtained c-TNS film in air at 500 °C for 3 hr (heating from 25 to 500 °C at a rate of 6.8 °C/min) using the oven.
    2. Repeat the sintering process twice.

3. **Preparation of Films**
    1. When the s-TNS films are immersed in solution, position the deposited s-TNS film so that it faces the top for all experimental procedures.
    2. Carry out all experiments under dark conditions by covering the setup with aluminum foil to avoid the photoreaction of TNS.

4. **Preparation of Methyl Viologen (MV^{2+}) Intercalated TNS Films (TNS/MV^{2+})**
    1. Immerse an s-TNS film in an aqueous solution of MV^{2+} dichloride salt (0.2 mM, 3 ml) in a Petri dish for 7 h at room temperature (RT) under dark conditions.
    2. Rinse the obtained samples with ultrapure water (5-10 ml) and dry in air at 60 °C using an oven in the dark for ~1 hr.

5. **Preparation of Au(III) Intercalated TNS Films (TNS/Au(III))**
    1. Immerse a TNS/MV^{2+} film in an aqueous solution of $HAuCl_4$ (25 mM, 3 ml) in a Petri dish for 3 hr at RT under dark conditions.
    2. Rinse the obtained samples with ultrapure water (5-10 ml) and dry in air at 60 °C using an oven in the dark for ~1 hr.

6. **Synthesis of AuNP within the Interlayer Space of TNS Films (TNS/AuNP)**
    1. Immerse a TNS/Au(III) film in an aqueous solution of $NaBH_4$ (0.1 M, 5 ml) in a Petri dish for 0.5 hr at RT under dark conditions.
    2. Dry the obtained films in air at 60 °C using an oven in the dark for ~1 hr.

7. **Preparation of $2\text{-}AET^+$ Intercalated TNS Films (TNS/$2\text{-}AET^+$)**
    1. Immerse an s-TNS film in an aqueous solution of $2\text{-}AET^+ Cl^-$ (0.1 M, 3 ml) in a Petri dish for 24 hr at RT.
    2. Rinse obtained films with ultrapure water (5-10 ml) and dry in air at 60 °C using an oven in the dark for ~1 hr.

8. **Au(III) and $2\text{-}AET^+$ Co-Intercalated TNS Films (TNS/$2\text{-}AET^+$/Au(III)).**
    1. Immerse a TNS/$2\text{-}AET^+$ film in an aqueous solution of $HAuCl_4$ (25 mM, 3 ml) for 3 h at RT.
    2. Rinse the obtained films with ultrapure water (5-10 ml) and dry in air at 60 °C using an oven in the dark for ~1 hr.

9. **Synthesis of AuNP within the Interlayer Space of TNS/$2\text{-}AET^+$ Films (TNS/$2\text{-}AET^+$/AuNP).**
    1. Immerse a TNS/$2\text{-}AET^+$/Au(III) film in an aqueous solution of $NaBH_4$ (0.1 M, 5 ml) in a Petri dish for 0.5 hr at RT under dark conditions.
    2. Rinse the obtained films with ultrapure water (5-10 ml) and dry in air at 60 °C using oven in the dark for ~1 hr.

10. **Characterizations**
    1. Carry out X-ray diffraction (XRD) analyses[21] using a desktop X-ray diffractometer with monochromatized Cu-K_α radiation (λ = 0.15405 nm), operated at 30 kV and 15 mA.
    2. Take energy dispersive X-ray spectrometry (EDS) spectra[21].

3. Employ a multichannel photodetector or steady-state ultraviolet-visible (UV-Vis) absorption spectrophotometer to record UV-Vis absorption spectra for the prepared samples using transmittance mode[21].

Representative Results

Two types of precursor films were used in this study (*i.e.,* with and without the protective reagent (2-AET^+) within the interlayer of TNS). In the absence of 2-AET^+, 1,1'-dimethyl-4,4'-bipyridinium dichloride (methyl viologen; MV^{2+}) was used as an expander of the interlayer space, because MV^{2+}-containing LMOSs have been frequently used as intermediates in the guest exchange method for preparing LMOSs[16,17,21,33-36].

Synthesis of AuNPs without 2-AET^+

To obtain the Au(III) intercalated TNS (TNS/Au(III)) film, an MV^{2+} intercalated TNS (TNS/MV^{2+})[21,24,25,27,29] film was soaked in an aqueous solution of $HAuCl_4$ (25 mM for 24 hr). Adsorption of gold species within the TNS was confirmed by energy dispersive X-ray spectrometry (EDS) analysis, which provided clear signals for Ti and Au; the atomic ratio of Ti:Au was estimated to be 1:0.08. Based on the chemical formula of the starting protonated, layered titanate ($H_{0.7}Ti_{1.825}O_4$) and the surface charge density (0.307-0.366 nm^2 per charge)[22], the area occupied by one Au atom was estimated to be 1.47-1.61 nm^2. Thus, a significant amount of Au atoms was accommodated within the TNS. In addition, an intense Cl K_α signal was detected, and the atomic ratio of Au:Cl was estimated to be 1:2.4 ± 0.1 on the EDS analysis (**Figure 2A**). This result implies that the unstable tetrachloroauric(III) acid was partly decomposed, and gold species were adsorbed on the TNS as decomposed products. However, the details of the decomposition and adsorption mechanisms of Au(III) are still unclear. We assume that Au(III) complexes with -OH groups, such as $AuCl_3(OH)$ and $AuCl_2(OH)_2$[37], were formed in the system, and -OH groups of Au species may assist with the adsorption of Au species within the interlayer of TNS through the interaction with the surface -OH groups of TNS[38]. The XRD profiles of the original TNS/MV^{2+} and TNS/Au(III) are shown in **Figures 3A** and **3B**, respectively. Further details of the XRD analysis (*i.e.,* diffraction angles, *d*(002) values, and full-width-at-half-maxima (FWHM) at *d*(002) signals of the investigated films) are also summarized in **Table 1**. Before being soaked in $HAuCl_4$ solution, two characteristic XRD signals were observed at 7.82° and 15.5° (*d* = 1.13 nm) for the TNS/MV^{2+} film, indicating that the film retains a stacking layer structure, as previously reported[21]. When the TNS/MV^{2+} film was soaked in $HAuCl_4$ solution, the two characteristic XRD signals were shifted to a higher angle region (*d* = 0.98 nm). The thickness of one layer of the TNS was reported to be 0.75 n [23,26,39,40], and thus, the estimated distance between the layers (clearance space; CLS) is 0.23 nm. This implies that MV^{2+} molecules within the interlayer space of the TNS were substituted by tetrachloroauric(III) acid or its decomposed products, as the ionic diameter of Au (~0.17 nm)[41-43] was smaller than that of MV^{2+} (molecular size: ~1.3 nm x 0.4 nm)[24]. Based on the EDS and XRD analyses, we can conclude that Au(III) species exist within the interlayer space of the TNS.

The obtained TNS/Au(III) films were treated with an aqueous $NaBH_4$ as a reductant, and the XRD profile of the $NaBH_4$-treated film is shown in **Figure 3C**. A characteristic *d*(002) = 1.00 nm diffraction signal was observed with a peak position nearly identical to that of the TNS/Au(III) film (**Table 1**). The $NaBH_4$-treated film exhibited a broader signal than that of the TNS/Au(III) film, suggesting that the regular stacking structure became disordered upon $NaBH_4$ treatment. These behaviors are quite similar to that observed for TNS and copper systems[21]. EDS analysis showed that the atomic ratio of Ti:Au was estimated to be 1:0.09, suggesting that gold species were not desorbed from TNS, even through the aqueous $NaBH_4$ treatment. Moreover, chloride atoms were not detected on EDS analysis (**Figure 1B**), suggesting that Au(III) species may be quantitatively reduced by $NaBH_4$. Upon treatment of the TNS/Au(III) film with $NaBH_4$, the color of the film immediately changed from clear to metallic purple, as shown in **Figure 4A** and **4B**. A new broad extinction (absorption and scattering) band at 400-600 nm was observed upon $NaBH_4$-treatment, as shown in **Figure 5**. This coloration of the films is consistent with the reduction of Au(III) to form AuNPs within the interlayer space of the TNS through the $NaBH_4$ treatment[21]. As-prepared $NaBH_4$-treated films were allowed to stand in an aerated $NaBH_4$ solution, and the color of the films gradually changed from metallic purple to a translucent dusty appearance within 30 min (**Figure 4C**). The characteristic extinction band at 400-600 nm also disappeared within 30 min, as shown in **Figure 5**[28]. Similar color changes were observed in both nitrogen- or oxygen-saturated aqueous $NaBH_4$ solutions, as shown in **Figure 6**. Since the color change was not suppressed under the nitrogen (N_2) atmosphere, the color change is not indicative of the oxidation of AuNPs within the interlayer of the TNS. This is in contrast to the copper and TNS systems[21]; CuNPs within the interlayer of the TNS were immediately oxidized by molecular oxygen. Thus, such a color change suggests aggregation of the AuNPs within the interlayer space of the TNS[28,44].

Synthesis of AuNPs with 2-AET^+ as a Protective Reagent

To avoid the aggregation of the AuNPs in the interlayer space of the TNS, the co-intercalation of 2-AET^+ and the gold species in TNS films was investigated, because alkylthiols and alkylammonium cations have been frequently used as protective reagents against the aggregation of AuNPs within homogeneous solutions[45,46] and the assistant reagents for intercalation compounds[16,17,34,47], respectively. To obtain the 2-AET^+ intercalated (TNS/2-AET^+) films, sintered TNS (s-TNS) films were soaked in 2-AET^+ aqueous solutions. The XRD profiles of the s-TNS and TNS/2-AET^+ films are shown in **Figure 1A** and **1B**, respectively. The starting s-TNS films exhibit characteristic *d*(002) signals at 9.92° (*d* = 0.89 nm). Upon treatment with aqueous 2-AET^+, the *d*(002) signal was shifted to a lower angle with *d* = 1.08 nm, and a new *d*(004) signal appeared. The CLS is estimated to be 0.33 nm (**Table 1**). Compared to the starting s-TNS film, the observed *d*(002) signal of TNS/2-AET^+ became intense and narrow, indicating that the stacking structures became ordered. These results suggest that 2-AET^+ molecules were intercalated into the TNS layer. The 2-AET^+ molecules might orient in an *anti-parallel* monolayer fashion and tilt with respect to the TNS sheet because the estimated CLS is slightly smaller than that for the molecular length of 2-AET^+ (~0.4 nm)[16,17]. The proposed structure of 2-AET^+-treated TNS (TNS/2-AET^+) is shown in **Figure 7A**.

The TNS/2-AET$^+$ films were soaked in $HAuCl_4$ aqueous solutions for 3 h, with the result that the characteristic *d*(002) signal shifted to a higher angle, indicating that shrinkage of the layer distance occurred (**Figure 1C** and **Table 1**). A significant amount of gold and chloride atoms were detected upon EDS analysis (Ti:Au = 1:0.02 and Au:Cl = 1:0.4), indicating that Au(III) atoms were intercalated in the TNS layer and that part of the starting tetrachloroauric(III) acid may have decomposed during the experimental procedures. The estimated CLS of the $HAuCl_4$-treated film was 0.25 nm, and the CLS was slightly smaller than that of the original TNS/2-AET$^+$ (Δd = 0.08 nm). However, the CLS was significantly larger than that of the ionic diameter of Au (~0.17 nm). Moreover, two broad and characteristic signals (3,100-3,200 and 3,300-3,450 cm^{-1}) that correspond to N-H stretching were detected in an FT-IR measurement. This result suggests that 2-AET$^+$ molecules remained in the interlayer space of TNS. XRD, EDS, and FT-IR analyses implied that both 2-AET$^+$ and Au(III) were intercalated within the interlayer of the TNS, and the proposed structure of the TNS containing 2-AET$^+$ and Au(III) (TNS/2-AET$^+$/Au(III)) is shown in **Figure 7B**.

TNS/2-AET$^+$/Au(III) films were soaked in the aqueous $NaBH_4$ solutions for 30 min, during which time the color of the film changed from clear to reddish, as shown in **Figure 8A**. The extinction and differential spectra of the $NaBH_4$-treated TNS/2-AET$^+$/Au(III) films are shown in **Figures 9** and **8B**, respectively. A clear extinction band at λ_{max} = 590 nm was observed upon $NaBH_4$ treatment, and the observed extinction band maximum was similar to that of the LSPR band of AuNP on TiO_2[5,48] or within the interlayer space of the TNS[28]. Tsukuda *et al.* have reported the formation of an Au(I)-thiolate complex[49]. However, we predicted that most Au atoms were fully reduced by $NaBH_4$ within the interlayer of TNS/2-AET$^+$ in the present state, because the extinction spectral shape was similar to that of independently synthesized Au(0) nanoparticles in the interlayer space of TNS[28]. Moreover, wide-angle XRD suggest that formation of crystalline gold species, as described below.

XRD analyses showed that the *d*(002) signals become broader and slightly shifted to a lower angle after the $NaBH_4$ treatment (**Figure 1D** and **Table 1**), suggesting that the regular stacking structure became disordered upon $NaBH_4$ treatment. The estimated atomic ratio of Ti:Au was 1:0.02, suggesting that gold species were not desorbed from TNS/2-AET$^+$ during the aqueous $NaBH_4$ treatment. These behaviors are quite similar to those observed for TNS/CuNPs and TNS/AuNPs, as previously described.

Wide-angle XRD profiles of various TNS films and the reflections corresponding to gold crystal (PDF: 00-001-1174) are shown in **Figure 10**. In the case of the starting s-TNS film, two weak diffraction signals corresponding to $Ti_{1.825}O_{0.175}$ sheets were observed at 37.8° and 48.2° (**Figure 10a**). The same diffraction signals were also observed for the TNS/2-AET$^+$ film with a peak position identical to that of the starting s-TNS film (**Figure 10b**). New characteristic XRD signals appeared at 38.3° and 44.5° for the $NaBH_4$-treated TNS/2-AET$^+$/Au(III) films, as shown in **Figure 10d**. However, the diffraction signals for the TNS sheets at 37.8° and 48.2° were retained and unchanged. The newly appeared XRD signals at 38.3° and 44.5° were quite similar to those for the *d*(111) and *d*(200) diffractions from crystalline gold. This result implies that crystalline gold (*i.e.,* AuNPs) were generated within the interlayer space of TNS. However, strangely, the two characteristic XRD signals appeared for the TNS/2-AET$^+$/Au(III) films, despite the non-treatment of $NaBH_4$ (**Figure 10c**), and the gold species should have remained as Au(III). Similar strange behaviors were also observed for TNS/Au(III) before and after $NaBH_4$ treatment, as shown in **Figure 11**. The origin of this behavior is not yet clear; however, we assume that the semiconductor and/or catalytic properties of TNS affect the Au-crystalline formation without $NaBH_4$ treatment, and perhaps light leaks or X-rays induce[50,51] the formation of a slight amount of reduced Au. Based on extinction, XRD, and EDS analyses, we can conclude that AuNPs formed within the interlayer space of TNS films (*i.e.,* TNS/2-AET$^+$/AuNP films) were successfully prepared through the presented procedure. Furthermore, the observed extinction band maximum suggests that AuNPs might be isolated. Thus, 2-AET$^+$ within the interlayer space of the TNS is considered an effective protection reagent for the AuNPs that form there.

The stability of AuNPs in the TNS layer with 2-AET$^+$ under ambient atmosphere was confirmed by extinction spectral analysis. The transmittance extinction and differential spectra of two types of TNS/2-AET$^+$/AuNP films (*i.e.,* as-prepared and within 5 min of $NaBH_4$ treatment, as well as after standing in an aerated atmosphere for 124 days under dark conditions) are shown in **Figure 12**. No spectral change was observed for the extinction spectra, even after 4 months, indicating that the AuNPs within the TNS with 2-AET$^+$ were stable against oxygen. Such stabilization of AuNPs within TNS films is expected to demonstrate great applicability in the development of cost-effective plasmonic catalysts.

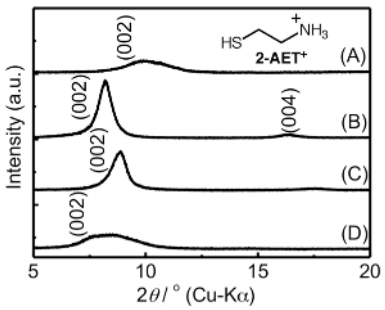

Figure 1: XRD profiles of the s-TNS (**A**), TNS/2-AET$^+$ (**B**), TNS/2-AET$^+$/Au(III) (**C**), and $NaBH_4$-treated TNS/2-AET$^+$/Au(III) (TNS/2-AET$^+$/AuNP) (**D**) films. Inset shows the chemical formula of 2-AET$^+$. Please click here to view a larger version of this figure.

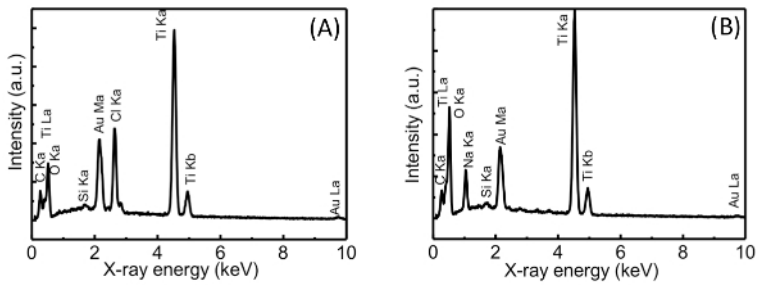

Figure 2: EDS spectra of the TNS/Au(III) (**A**) and $NaBH_4$-treated TNS/Au(III) (**B**) films. Please click here to view a larger version of this figure.

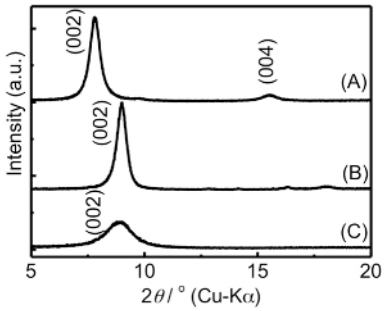

Figure 3: XRD profiles of the TNS/MV^{2+} (**A**), TNS/Au(III) (**B**), and $NaBH_4$-treated TNS/Au(III) (**C**) films. Please click here to view a larger version of this figure.

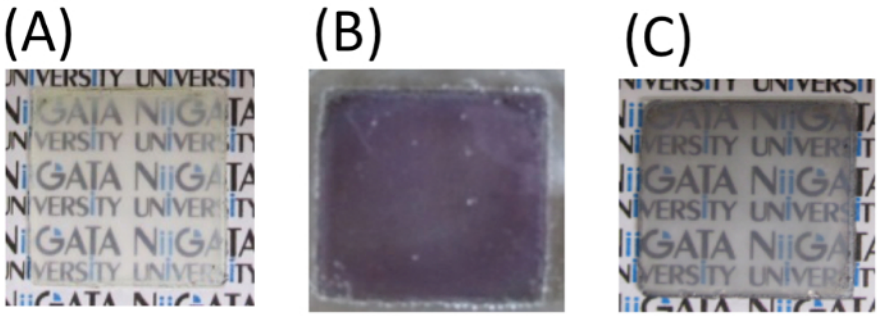

Figure 4: Photographs of various TNS and gold hybrid films: TNS/Au(III) (**A**) and $NaBH_4$-treated TNS/Au(III) films within 1 min (**B**) and 30 min (**C**) in aerated $NaBH_4$ aqueous solutions. Please click here to view a larger version of this figure.

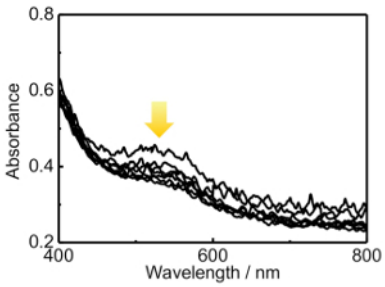

Figure 5.: Extinction spectral changes of the $NaBH_4$-treated TNS/Au(III) films in aerated $NaBH_4$ solution for 1-30 min. The arrow indicates the disappearance of extinction bands at 400-600 nm. Please click here to view a larger version of this figure.

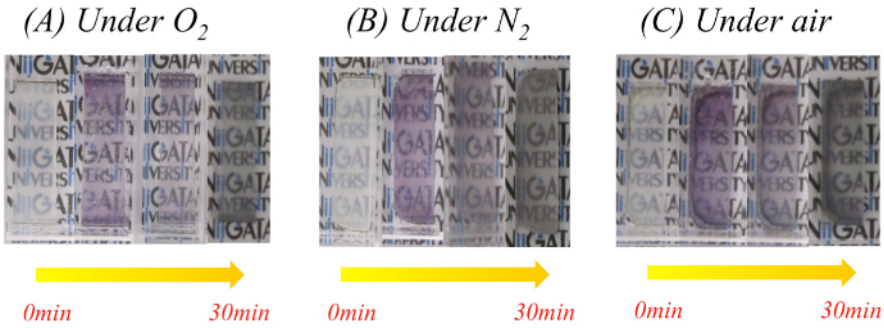

Figure 6: Photographs of the $NaBH_4$-treated TNS/Au(III) films in various gas-saturated $NaBH_4$ aqueous solutions: (**A**) oxygen, (**B**) nitrogen, and (**C**) air. Please click here to view a larger version of this figure.

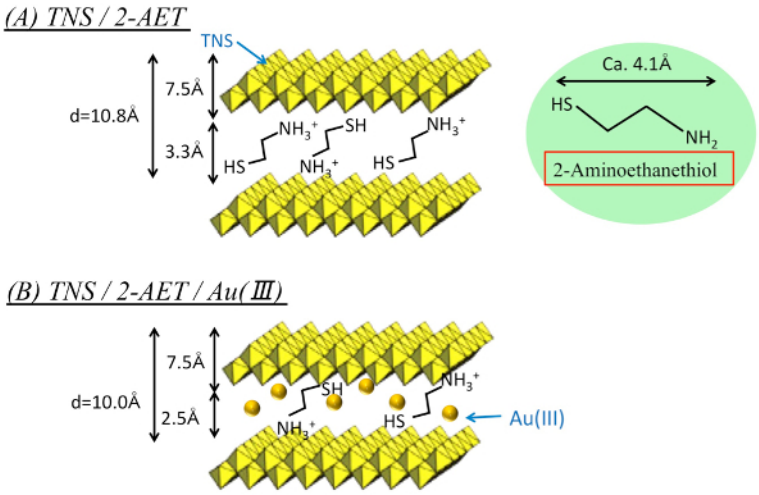

Figure 7: Proposed schematic of the TNS/2-AET^+ (**A**) and $HAuCl_4$-treated TNS/2-AET^+ (TNS/2-AET^+/Au(III)) (**B**) films. Please click here to view a larger version of this figure.

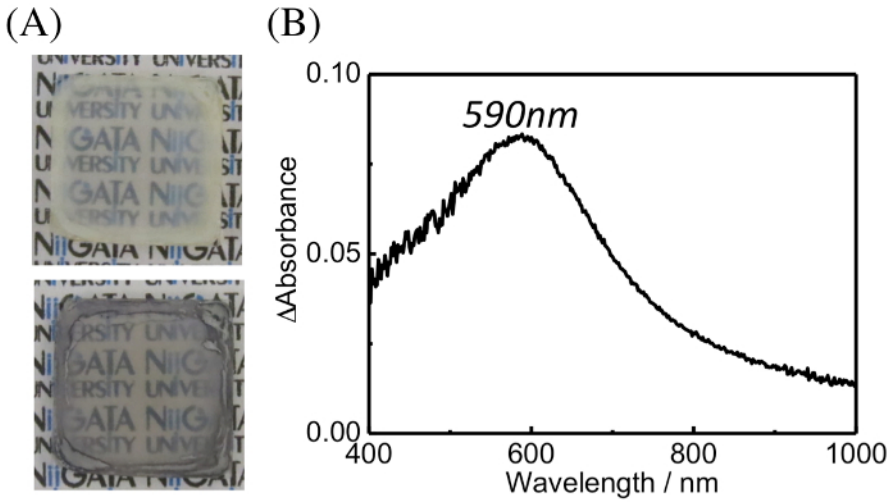

Figure 8: (**A**) Photograph of the TNS/2-AET^+/Au(III) (top) and $NaBH_4$-treated films (bottom). (**B**) Differential extinction spectrum of the $NaBH_4$-treated TNS/2-AET^+/Au(III) film. The spectrum was normalized by considering the TNS/2-AET^+/Au(III) film as the background spectrum and subtracting it from the spectrum obtained after $NaBH_4$ treatment. Please click here to view a larger version of this figure.

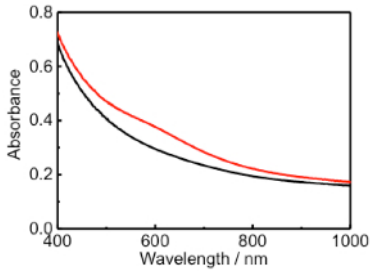

Figure 9: Transmittance extinction spectra of the TNS/2-AET$^+$/Au(III) (black) and $NaBH_4$-treated TNS/2-AET$^+$/Au(III) (red) films. Please click here to view a larger version of this figure.

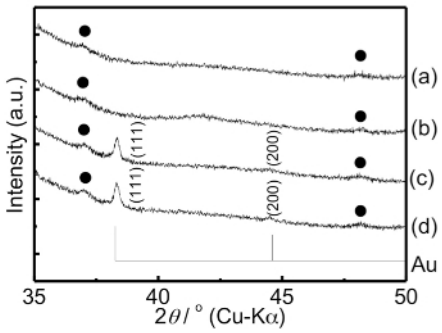

Figure 10: Wide-angle XRD profiles of the s-TNS (**a**), TNS/2-AET$^+$ (**b**), TNS/2-AET$^+$/Au(III) (**c**), and $NaBH_4$-treated TNS/2-AET$^+$/Au(III) (**d**) films, as well as the PDF index of crystalline gold. Solid circles indicate diffractions from $Ti_{1.825}O_{0.175}$ sheets. Please click here to view a larger version of this figure.

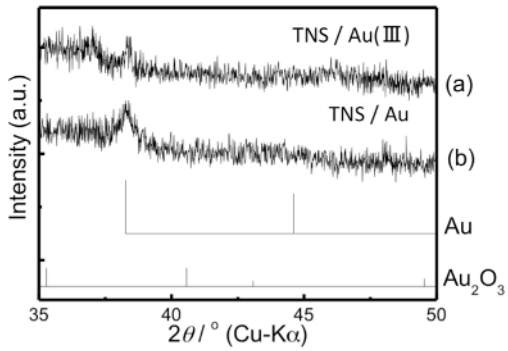

Figure 11: Wide-angle XRD profiles of the TNS/Au(III) (**a**) and $NaBH_4$-treated TNS/Au(III) (**b**) films. Please click here to view a larger version of this figure.

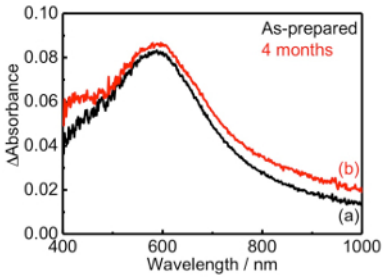

Figure 12: Differential extinction spectra of TNS/2-AET$^+$/AuNP films: as-prepared (**a**) and after standing under aerated and dark conditions for 124 days (**b**). The spectra were normalized by subtracting TNS/2-AET$^+$/Au(III) film as the background spectrum. Please click here to view a larger version of this figure.

	2θ / °	*d*(002) / nm	FWHM / °	CLS[a)] / nm
s-TNS	9.92	0.89	2.13	0.14
TNS/MV^{2+}	7.82, 15.5	1.13	0.55	0.38
TNS/Au(III)	8.99, 18.0	0.98	0.52	0.23
TNS/AuNP	8.86	1.00	1.37	0.25
TNS/2-AET^+	8.18, 16.3	1.08	0.73	0.33
TNS/2-AET^+/ Au(III)	8.88, 17.6	1.00	0.80	0.25
TNS/2-AET^+/AuNP	8.19	1.08	2.31	0.33

a) Clearance space can be defined as the value obtained by subtraction of the intrinsic thickness of TNS sheet (0.75 nm)[23,26,39,40] from the observed *d*(002) distance.

Table 1: Diffraction angles (2θ), *d* values, FWHM of *d*(002) signals on the XRD profiles, and estimated clearance spaces (CLSs) of the invested films.

Discussion

This manuscript provides a detailed protocol for the *in situ* synthesis of gold nanoparticles (AuNPs) within the interlayer space of TNS films. This is the first report of the *in situ* synthesis of AuNPs within the interlayer space of TNS. Moreover, we found that the 2-AET^+ works as an effective protective reagent for AuNPs within the interlayer of TNS. These methods hybridized AuNPs and TNS transparent films. TNS films with good optical transparency[21] were synthesized through sintering processes (s-TNS films), as presented in the protocol section. The sintering processes are required repeatedly for the complete removal of organic impurities. When the organic impurities remain, the films turn dark gray. Here, the sintering processes were repeated twice as a typical run; however, further repetitions are permissible.

We successfully synthesized AuNP-containing layered TNS films using two intermediate films (*i.e.,* TNS/MV^{2+} and TNS/2-AET^+ films). The two intermediate films were soaked in an aqueous $HAuCl_4$ solution, and considerable amounts of gold species (the occupied space of one Au atom was 1.47-1.61 nm^2) were accommodated within the interlayer spaces of the TNS films. This suggests that the MV^{2+} and 2-AET^+ molecules act as effective expanders of the TNS layers (**Figures 1B** and **2A** and **Table 1**). However, detailed adsorption mechanisms of gold species into the interlayer of TNS are still unclear.

The obtained Au(III)-containing films were soaked in an aqueous $NaBH_4$ solution, and the color of the films immediately changed from clear to purple (**Figures 4** and **6**), suggesting the formation of AuNPs within the TNS interlayer. Moreover, the AuNP-containing TNS films maintain good optical transparency (see **Figure 8A** as a typical example) and cohesion against the glass substrate, even when soaked in aqueous MV^{2+}, 2-AET^+, and $NaBH_4$ solutions. These methods can apply to other metal ions, such as copper and silver[21].

When the TNS/MV^{2+} film was used as the intermediate, the color of the AuNPs changed within 30 min (**Figure 6**), suggesting the aggregation of AuNPs within the interlayer space of the TNS. However, the aggregation and color change of the AuNPs were effectively suppressed using the TNS/2-AET^+ film as the intermediate (**Figure 8**). This suggests that 2-AET^+ molecules work as effective protective reagents for AuNPs within TNS interlayers, similar to the AuNPs in solution.

The synthesized TNS/2-AET^+/AuNPs were stable against oxygen and the characteristic extinction band at 590 nm was maintained beyond 4 months. Such properties and stabilities of AuNPs within TNS interlayers are expected to demonstrate applicability in catalysis, photocatalysis, and the development of cost-effective plasmonic devices.

Disclosures

We have nothing to disclose.

Acknowledgements

This work was partly supported by Nippon Sheet Glass Foundation for Materials Science and Engineering and JSPS KAKENHI (Grant-in-Aid for Challenging Exploratory Research, #50362281).

References

1. Kelly, K. L., Coronado, E., Zhao, L. L., & Schatz, G. C. The Optical Properties of Metal Nanoparticles: The Influence of Size, Shape, and Dielectric Environment. *J. Phys. Chem. B.* **107** (3), 668-677 (2003).
2. Rycenga, M. *et al.* Controlling the Synthesis and Assembly of Silver Nanostructures for Plasmonic Applications. *Chem. Rev.* **111** (6), 3669-3712 (2011).
3. The Binh, N. *et al.* Preparation of metal nanoparticles for surface enhanced Raman scattering by laser ablation method. *Adv. Nat. Sci.: Nanosci. Nanotechnol.* **3** (2), 025016 (2012).
4. Chen, H., Shao, L., Li, Q., & Wang, J. Gold nanorods and their plasmonic properties. *Chem. Soc. Rev.* **42** (7), 2679-2724 (2013).
5. Subramanian, V., Wolf, E. E., & Kamat, P. V. Influence of Metal/Metal Ion Concentration on the Photocatalytic Activity of TiO2−Au Composite Nanoparticles. *Langmuir.* **19** (2), 469-474 (2003).

6. Linic, S., Christopher, P., & Ingram, D. B. Plasmonic-metal nanostructures for efficient conversion of solar to chemical energy. *Nat Mater.* **10** (12), 911-921 (2011).
7. Gomes Silva, C., Juárez, R., Marino, T., Molinari, R., & García, H. Influence of Excitation Wavelength (UV or Visible Light) on the Photocatalytic Activity of Titania Containing Gold Nanoparticles for the Generation of Hydrogen or Oxygen from Water. *J. Am. Chem. Soc.* **133** (3), 595-602 (2011).
8. Hou, W. *et al.* Photocatalytic Conversion of CO2 to Hydrocarbon Fuels via Plasmon-Enhanced Absorption and Metallic Interband Transitions. *ACS Catal.* **1** (8), 929-936 (2011).
9. Wang, W.-N. *et al.* Size and Structure Matter: Enhanced CO2 Photoreduction Efficiency by Size-Resolved Ultrafine Pt Nanoparticles on TiO2 Single Crystals. *J. Am. Chem. Soc.* **134** (27), 11276-11281 (2012).
10. Shi, X., Ueno, K., Takabayashi, N., & Misawa, H. Plasmon-Enhanced Photocurrent Generation and Water Oxidation with a Gold Nanoisland-Loaded Titanium Dioxide Photoelectrode. *J. Phys. Chem. C.* **117** (6), 2494-2499 (2013).
11. Tanaka, A., Sakaguchi, S., Hashimoto, K., & Kominami, H. Preparation of Au/TiO2 with Metal Cocatalysts Exhibiting Strong Surface Plasmon Resonance Effective for Photoinduced Hydrogen Formation under Irradiation of Visible Light. *ACS Catal.* **3** (1), 79-85 (2013).
12. Bian, Z., Tachikawa, T., Zhang, P., Fujitsuka, M., & Majima, T. Au/TiO2 Superstructure-Based Plasmonic Photocatalysts Exhibiting Efficient Charge Separation and Unprecedented Activity. *J. Am. Chem. Soc.* **136** (1), 458-465 (2014).
13. Ide, Y. *et al.* Hybridization of Au nanoparticle-loaded TiO2 with BN nanosheets for efficient solar-driven photocatalysis. *J. Mater. Chem. A.* **2** (12), 4150-4156 (2014).
14. Zheng, Z., Tachikawa, T., & Majima, T. Plasmon-induced spatial electron transfer between single Au nanorods and ALD-coated TiO2: dependence on TiO2 thickness. *Chem. Commun.* **51** (76), 14373-14376 (2015).
15. Inui, Y. *et al.* Reversible redox processes of poly(anilines) in layered semiconductor niobate films under alternate UV-Vis light illumination. *J. Phys. Chem. B.* **111** (42), 12162-12169 (2007).
16. Yui, T., & Takagi, K. in *Bottom-up Nanofabrication.* Vol. 5 eds Katsuhiko Ariga & Hari Singh Nalwa) Ch. 2, 35-90 American Scientific Publishers (2009).
17. Sasai, R., Yui, T., & Takagi, K. in *Encyclopedia of Nanoscience and Nanotechnology.* Vol. 24 (ed Hari Singh Nalwa) 303-361 American Scientific Publishers (2011).
18. Yui, T. *et al.* Visible light-induced electron transfers in titania nanosheet and mesoporous silica integrated films. *Bull. Chem. Soc. Jpn.* **79** (3), 386-396 (2006).
19. Yui, T. *et al.* Photoinduced one-electron reduction of MV2+ in titania nanosheets using porphyrin in mesoporous silica thin films. *Langmuir.* **21** (7), 2644-2646 (2005).
20. Yui, T. *et al.* Remarkably stabilized charge separations in inorganic nanospace. *Bull. Chem. Soc. Jpn.* **82** (7), 914-916 (2009).
21. Sasaki, K. *et al.* Synthesis of copper nanoparticles within the interlayer space of titania nanosheet transparent films. *J. Mater. Chem. C.* **4** (7), 1476-1481 (2016).
22. Sasaki, T., Komatsu, Y., & Fujiki, Y. A new layered hydrous titanium dioxide HTi2 -/4O4[middle dot]H2O. *J. Chem. Soc., Chem. Commun.* (12), 817-818 (1991).
23. Sasaki, T., & Watanabe, M. Osmotic Swelling to Exfoliation. Exceptionally High Degrees of Hydration of a Layered Titanate. *J. Am. Chem. Soc.* **120** (19), 4682-4689 (1998).
24. Yui, T. *et al.* Synthesis of photofunctional titania nanosheets by electrophoretic deposition. *Chem. Mater.* **17** (1), 206-211 (2005).
25. Tachikawa, T., Yui, T., Fujitsuka, M., Takagi, K., & Majima, T. Photocatalytic electron transfer in hybrid titania nanosheets studied by nanosecond laser flash photolysis. *Chem. Lett.* **34** (11), 1522-1523 (2005).
26. Zhou, Y., Ma, R., Ebina, Y., Takada, K., & Sasaki, T. Multilayer Hybrid Films of Titania Semiconductor Nanosheet and Silver Metal Fabricated via Layer-by-Layer Self-Assembly and Subsequent UV Irradiation. *Chem. Mater.* **18** (5), 1235-1239 (2006).
27. Yui, T. *et al.* Photochemical electron transfer though the interface of hybrid films of titania nano-sheets and mono-dispersed spherical mesoporous silica particles. *Phys. Chem. Chem. Phys.* **8** (39), 4585-4590 (2006).
28. Sakai, N., Sasaki, T., Matsubara, K., & Tatsuma, T. Layer-by-layer assembly of gold nanoparticles with titania nanosheets: control of plasmon resonance and photovoltaic properties. *J. Mater. Chem.* **20** (21), 4371-4378 (2010).
29. Yui, T. *et al.* Photoinduced Electron Transfer between the Anionic Porphyrins and Viologens in Titania Nanosheets and Monodisperse Mesoporous Silica Hybrid Films. *ACS Appl. Mater. Interfaces.* **3** (4), 931-935 (2011).
30. Wang, L., & Sasaki, T. Titanium Oxide Nanosheets: Graphene Analogues with Versatile Functionalities. *Chem. Rev.* **114** (19), 9455-9486 (2014).
31. Eguchi, M., Ito, M., & Ishibashi, T.-a. Stabilization and Modification of Gold Nanocube Surfaces with Layered Silicate. *Chem. Lett.* **43** (1), 140-142 (2014).
32. Fujimura, T., Yoshida, Y., Inoue, H., Shimada, T., & Takagi, S. Dense Deposition of Gold Nanoclusters Utilizing a Porphyrin/Inorganic Layered Material Complex as the Template. *Langmuir.* **31** (33), 9142-9147 (2015).
33. Tong, Z., Shichi, T., & Takagi, K. Visible-Light Induced Charge-Separation between Consecutively Cast Porphyrin and Methyl Viologen Multilayered Titanoniobate Hybrid Films. *J. Phys. Chem. B.* **106** (51), 13306-13310 (2002).
34. Tong, Z., Shichi, T., Oshika, K., & Takagi, K. A Nanostructured Hybrid Material Synthesized by the Intercalation of Porphyrin into Layered Titanoniobate. *Chem. Lett.* **31** (9), 876-877 (2002).
35. Tong, Z., Takagi, S., Tachibana, H., Takagi, K., & Inoue, H. Novel Soft Chemical Method for Optically Transparent Ru(bpy)3-K4Nb6O17 Thin Film. *J. Phys. Chem. B.* **109** (46), 21612-21617 (2005).
36. Hattori, T. *et al.* Hybridization of layered niobates with cationic dyes. *Res. Chem. Intermed.* **32** (7), 653-669 (2006).
37. Moreau, F., Bond, G. C., & Taylor, A. O. Gold on titania catalysts for the oxidation of carbon monoxide: control of pH during preparation with various gold contents. *J. Catal.* **231** (1), 105-114 (2005).
38. Ivanova, S., Petit, C., & Pitchon, V. A new preparation method for the formation of gold nanoparticles on an oxide support. *Appl. Cat. A.* **267** (1-2), 191-201 (2004).
39. Sasaki, T., Watanabe, M., Hashizume, H., Yamada, H., & Nakazawa, H. Macromolecule-like Aspects for a Colloidal Suspension of an Exfoliated Titanate. Pairwise Association of Nanosheets and Dynamic Reassembling Process Initiated from It. *J. Am. Chem. Soc.* **118** (35), 8329-8335 (1996).
40. Tanaka, T., Ebina, Y., Takada, K., Kurashima, K., & Sasaki, T. Oversized Titania Nanosheet Crystallites Derived from Flux-Grown Layered Titanate Single Crystals. *Chem. Mater.* **15** (18), 3564-3568 (2003).
41. *Denkikagaku Binran.* 5th edn, Maruzen (2000).

42. Shannon, R. D. Revised effective ionic radii and systematic studies of interatomic distances in halides and chalcogenides. *Acta Cryst.* **A32** 751-767 (1976).
43. Jia, Y. Q. Crystal radii and effective ionic radii of the rare earth ions. *J. Solid State Chem.* **95** (1), 184-187 (1991).
44. Grabar, K. C., Freeman, R. G., Hommer, M. B., & Natan, M. J. Preparation and Characterization of Au Colloid Monolayers. *Anal. Chem.* **67** (4), 735-743 (1995).
45. Niidome, T., Nakashima, K., Takahashi, H., & Niidome, Y. Preparation of primary amine-modified gold nanoparticles and their transfection ability into cultivated cells. *Chem. Commun.* (17), 1978-1979 (2004).
46. Kawano, T., Horiguchi, Y., Niidome, Y., Niidome, T., & Yamada, S. Preparation of Cationic Gold Nanoparticle in Aqueous Solutions of 2-Aminoethanethiol Hydrochloride. *Bunseki Kagaku.* **54** (6), 521-526 (2005).
47. Tong, Z., Shichi, T., Kasuga, Y., & Takagi, K. The Synthesis of Two Types of Layered Niobate Hybrid Materials by the Selective Intercalation of Ionic Porphyrin. *Chem. Lett.* **31** (12), 1206-1207 (2002).
48. Zhao, S., Chen, S., Wang, S., & Quan, Z. Composite Au/TiO2 Nanoparticles: Synthesis, Characterization, and Assembly by Using Potentiostatic Technique. *J. Colloid Interface Sci.* **221** (2), 161-165 (2000).
49. Negishi, Y., Nobusada, K., & Tsukuda, T. Glutathione-Protected Gold Clusters Revisited: Bridging the Gap between Gold(I)−Thiolate Complexes and Thiolate-Protected Gold Nanocrystals. *J. Am. Chem. Soc.* **127** (14), 5261-5270 (2005).
50. Schmidt-Stein, F. *et al.* X-ray induced photocatalysis on TiO2 and TiO2 nanotubes: Degradation of organics and drug release. *Electrochem. Commun.* **11** (11), 2077-2080 (2009).
51. Tamura, K. *et al.* X-ray induced photoelectrochemistry on TiO2. *Electrochim. Acta.* **52** (24), 6938-6942 (2007).

